Maritime Targets Detection from Ground Cameras Exploiting Semi-supervised Machine Learning

Eftychios Protopapadakis[1], Konstantinos Makantasis[1] and Nikolaos Doulamis[2]
[1]*Technical University of Crete, Chania, Greece*
[2]*National Technical University of Athens, Athens, Greece*

Keywords: Vision-based System, Maritime Surveillance, Semi-supervised Learning, Visual Attention Maps, Vehicle Tracking.

Abstract: This paper presents a vision-based system for maritime surveillance, using moving PTZ cameras. The proposed methodology fuses a visual attention method that exploits low-level image features appropriately selected for maritime environment, with appropriate tracker. Such features require no assumptions about environmental nor visual conditions. The offline initialization is based on large graph semi-supervised technique in order to minimize user's effort. System's performance was evaluated with videos from cameras placed at Limassol port and Venetian port of Chania. Results suggest high detection ability, despite dynamically changing visual conditions and different kinds of vessels, all in real time.

1 INTRODUCTION

Management of emergency situations, known to the maritime domain, can be supported by advanced surveillance systems suitable for complex environments. Such systems vary from radar-based to video-based. The former, however, has two major drawbacks (Zemmari et al., 2013); it is quite expensive and its performance is affected by various factors (e.g. echoes from targets out of interest). The latter, consists of various techniques, each one with specific advantages and drawbacks. The majority of such systems are are controlled by humans, who are responsible for monitoring and evaluating numerous video feeds simultaneously.

Advanced surveillance systems should process and present collected sensor data, in an intelligent and meaningful way, to give a sufficient information support to human decision makers (Fischer and Bauer, 2010). The detection and tracking of vessels is inherently depended on dynamically varying visual conditions (e.g. varying lighting and reflections of sea). So, to successfully design a vision-based surveillance system, we have to carefully define both its operation requirements and vessels' characteristics.

On the one hand there are minimum standards concerning operation requirements (Szpak and Tapamo, 2011). At first, it must determine possible targets within a scene containing a complex, moving background. Additionally, the system must not produce false negatives and keep as low as possible the number of false positives. Since we are talking about surveillance system, it must be fast and highly efficient, operating at a reasonable frame rate and for long time periods using a minimal number of scene-related assumptions.

On the other hand, regardless of vessel types variation, there are four major descriptive categories. First comes the size, which ranges from jet-skis to large cruise ships. Secondly, we have the moving speed. Thirdly, vessels move to any direction, according to the camera position, and thus their angle varies from $0^{\circ}$to 360°. Finally, there is vehicles' visibility. Some vessels have a good contrast to the sea water while others are intentionally camouflaged. A robust maritime surveillance system must be able to detect vessels having any of the above properties.

1.1 Related Work

This paper focuses on detection and tracking of targets within camera's range, rather than their trajectory patterns' investigation (Lei, 2013; Vandecasteele et al., 2013) or their classification in categories of interest (Maresca et al., 2010). The system's main purpose is to support end-user in monitoring coastlines, regardless of existing conditions.

Object detection is a common approach with

Protopapadakis E., Makantasis K. and Doulamis N..
Maritime Targets Detection from Ground Cameras Exploiting Semi-supervised Machine Learning.
DOI: 10.5220/0005456205830594
In *Proceedings of the 10th International Conference on Computer Vision Theory and Applications* (MMS-ER3D-2015), pages 583-594
ISBN: 978-989-758-090-1

mayny variations; i.e. an-isotropic diffusion (Voles, 1999), which has high computational cost and performs well only for horizontal and vertical edges, foreground object detection /image color segmentation fusion (Socek et al., 2005). In (Albrecht et al., 2011a; Albrecht et al., 2010) a maritime surveillance system mainly focuses on finding regions in images, where is a high likelihood of a vessel being present, is proposed. Such system was expanded by adding a sea/sky classification approach using HOG (Albrecht et al., 2011b). Vessel classes detection, using a trained set of MACH filters was proposed by (Rodriguez Sullivan and Shah, 2008).

All of the above approaches adopt offline learning methods that are sensitive to accumulation errors and difficult to generalize for various operational conditions. (Wijnhoven et al., 2010) utilized an online trained classifier, based on HOG. However, retraining takes place when a human user manually annotates the new training set. In (Szpak and Tapamo, 2011) an adaptive background subtraction technique is proposed for vessels extraction. Unfortunately, when a target is almost homogeneous is difficult, for the background model, to learn such environmental changes without misclassifying the target.

More recent approaches, using monocular video data, are the works (Makantasis et al., 2013) and (Kaimakis and Tsapatsoulis, 2013). The former, utilizes a fusion of Visual Attention Map (VAM) and background subtraction algorithm, based on Mixture Of Gaussians (MOG), to produce a refined VAM. These features are fed to a neural network tracker, which is capable of online adaptation. The latter, utilized statistical modelling of the scene's non-stationary background to detect targets implicitly.

The work of (Auslander et al., 2011) emphasize on algorithms that automatically learn anomaly detection models for maritime vessels, where the tracks are derived from ground-based optical video, and no domain-specific knowledge is employed. Some models can be created manually, by eliciting anomaly models in the form of rules from experts (Nilsson et al., 2008), but this may be impractical if experts are not available, cannot easily provide these models, or the elicitation cost may be high.

1.2 Our Contribution

A careful examination of the proposed methodologies suggest that specific points have to be addressed. Firstly, a system needs to combine both supervised and unsupervised tracking techniques, in order to exploit all the possible advantages. Secondly, since we deal with vast amount of available data, we need to reduce, as much as possible, the required effort for the initialization of the system.

The innovation of this paper lies in the creation of a visual detection system, able to overcome the aforementioned difficulties by combining various, well tested techniques and, at the same time, minimizes effort during the offline initialization using a Semi-Supervised Learning (SSL) technique, appropriate for large data sets.

In contrast to the approach of (Makantasis et al., 2013), the user has to roughly segment few images, i.e. use minimal effort, in order to create an initial training set. Such procedure is easily implemented using the suggested areas according to the unsupervised techniques' results. Collaboration of visual attention maps, that represents the probability of a vessel being present in the scene, and background subtraction algorithms provides to the user initially segmented parts, over which user further actuates.

Then, SVMs are used as the additional supervised technique, in order to handle new video frames. The significant amount of labelled data for the training process originates from the previously generated roughly segmented data sets. In order to facilitate the creation of such training set and further refine it (i.e. correct some user errors), SSL graph-based algorithms need to be involved.

Unfortunately, SSL techniques scale badly as the available data rises. To make matters worse, (Nadler et al., 2009) have shown that graph laplacian methods (and more specific the regularization approach (Zhu, 2003) and the spectral approach (Belkin and Niyogi, 2002)) are not well posed in spaces $\mathbb{R}^d$, $d \geq 2$, and as the number of unlabelled points increases the solution degenerates to a non-informative function. Consequently, a semi-supervised procedure, suitable for large data sets is exploited for the offline initialization, significantly reducing the effort required.

The rest of the paper is organized as follows: Section 2 presents the system's structure, suitable for the maritime surveillance problem. Section 3 describes the procedure followed for the construction of feature vectors, capable to characterize the pixels of a frame. Section 4 explains how target detection is performed using pixel-wise binary classification technique. Finally, in section 5, an excessive study on system's results is presented.

2 THE PROPOSED SYSTEM

2.1 System Architecture

The goal of the presented system is the real-time detection and tracking of maritime targets. Towards this direction, an *appearance-based* approach is adopted to create visual attention maps that represent the probability of a target being present in the scene. High probability implies high confidence for a maritime target's presence.

Visual attention maps creation is based exclusively on each frame's visual content, in relation to their surrounding regions or the entire image. Due to this limitation, high probability is assigned, frequently, to image regions that depict non-maritime targets (e.g. stationary land parts). In order to overcome such drawback, our system exploits the temporal relationship between subsequent frames. Concretely, video blocks, containing a predefined number, h, of frames and covering a time span, T, are used to model the pixels' intensities.

Thus, the temporal evolution of pixels intensities is utilized to estimate a pixel-wise background model, capable to denote each one of the pixels of the scene as background or foreground. By using a background modelling algorithm, system can efficiently discriminate moving from stationary objects in the scene. In order to model pixels' intensities, we use the background modelling algorithm presented in (Zivkovic, 2004). This choice is justified by the fact that this algorithm can automatically fully adapt to dynamically changing visual conditions and cluttered background.

Let us denote as $p_{xy}^{(i)}$ the pixel of a frame i at location (x,y) on image plane. Having constructed the visual attention maps and applied background modeling algorithm, the pixel $p_{xy}^{(i)}$ is described by a feature vector $\boldsymbol{f}_{xy}^{(i)}$: $\boldsymbol{f}_{xy}^{(i)} = [f_{1,xy}^{(i)} \cdots f_{k,xy}^{(i)}]^T$, where $f_{1,xy}^{(i)}, \ldots, f_{k-1,xy}^{(i)}$ stand for scalar features that correspond to the probabilities assigned to the pixel $p_{xy}^{(i)}$ by different visual attention maps, while $f_{k,xy}^{(i)}$ is the binary output of background modeling algorithm, associated with the same pixel. In order to detect maritime targets, these features are fed to a binary classifier which classifies pixels into two disjoint classes, C_T and C_B.

If we denote as $Z^{(i)} = C_T^{(i)} \cup C_B^{(i)}$ the set that contains all pixels of frame i, then the first class, $C_T^{(i)}$, contains all pixels that depict a part of a maritime target, while the second class, $C_B^{(i)}$, equals to $Z^{(i)} - C_T^{(i)}$. We used SVMs to transact the classification task for the proposed maritime surveillance system. Selection of the SVM, over other supervised classification methods, is justified by its robustness, when handling unbalanced classes.

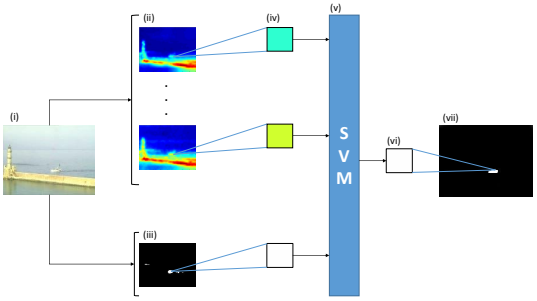

Figure 1: System's architecture illustration. Image in (i), corresponds to the original captured frame. In (ii), the output of visual attention maps is presented. High probability is represented with red color, while low probability with deep blue. The output of background modeling algorithm is shown in (iii). The column in (iv) represents a feature vector for a specific pixel, which is fed to a binary classifier (v). The output of the classifier in pixel level is presented in (vi) and in frame level in (vii).

The overall architecture of the proposed maritime surveillance system is presented in Fig.1. Initially, the original captured frame, Fig.1(i), is processed to extract pixel-wise features using visual attention maps, Fig.1(ii), and background modelling, Fig.1(iii). Then the feature vector of each one pixel, Fig.1(iv), is processed by a binary classifier, Fig.1(v), who decides if the pixel corresponds to a part of a maritime target, Fig.1(vi). The classifier's output in frame-level is shown in Fig.1(vii).

2.2 Problem Formulation

Maritime target detection can be seen as an image classification problem. Thus, we classify each one of the frame's pixels in one of two classes, C_T and C_B. If we denote as $l_{xy}^{(i)}$ the label of pixel $p_{xy}^{(i)}$, then, for a frame i, the classification task can be formulated as:

$$l_{xy}^{(i)} = \begin{cases} 1 \text{ if } p_{xy}^{(i)} \in C_T \\ -1 \text{ if } p_{xy}^{(i)} \in C_B \end{cases} \quad (1)$$

where $x = 1,\ldots,w$, $y = 1,\ldots,h$ and h,w stand for frame's height and width.

The SVM classifier will be formed through a training process, which requires the formation of a robust training set composed of pixels, along with their associated labels. Such a set can be formed by the user, through a rough segmentation of a frame t into two regions, that contain positive and negative samples, i.e. $C_T^{(t)}$ class labelled with 1 and $C_B^{(t)}$ class labelled with -1. The union of $C_T^{(t)}$ and $C_B^{(t)}$ consists the initial training set S.

At this point in the training set S, each pixel is described only by its intensity, which does not provide sufficient information for separating pixels into two disjoint classes. Taking into consideration the application domain, which indicates that the largest part of a frame will depict sea and sky, we exploit low level features to emphasize man-made structures in the scene.

Then, visual attention maps are created, which indicate the probability a pixel to depict a part of a maritime target. In addition, based on the observation that a vessel must be depicted as a moving object, we implicitly capture the presence of motion by exploiting a background modeling algorithm. Using the output of visual attention maps and the background modeling algorithm, each pixel is described by the feature vector of sec.2.1 and the training set S can be transformed to: $S = \{(\boldsymbol{f}_{xy}^{(t)}, l_{xy}^{(t)})\}$ for $x = 1,...,w$ and $y = 1,...,h$.

Although the elements of S are labelled by a human user, the labelling procedure may contain inconsistencies. This is mainly caused by the fact that human centric labelling, especially of image data, is an arduous and inconsistent task, due to the complexity of the visual content and the huge manual effort required.

In order to overcome this drawback, we refine the initial training set by i) selecting the most *representative* samples from each class and ii) labelling the rest of the samples using a *semi-supervised* algorithm. Selection of the most representative samples is taken place py applying simplex volume expansion on the samples of each class separately. Then representative samples are used by the semi-supervised algorithm as landmarks, in order to label the rest of the samples. Using the refined training set, the binary classifier can be successfully trained to classify the pixels of subsequent frames, addressing this way the initial classification problem of Eq.1.

3 PIXEL-WISE VISUAL DESCRIPTION

In this section we describe the procedure for constructing feature vectors, capable to characterize the pixels of a frame. The whole process is tuned for maritime imagery and is guided by the operational requirements that an accurate and robust maritime surveillance system must fulfil. Feature vectors are created for each pixel.

3.1 Scale Invariance

Potential targets in maritime environment vary in sizes, either due to their physical size or due to the distance between them and the camera. Despite that, most of the feature detectors operate as kernel based method and thus they prefer objects of a certain size. As presented in (Alexe et al., 2010) and (Liu et al., 2011) images must be represented in different scales in order to overcome this limitation. In our approach, a Gaussian image pyramid is exploited in order to provide scale invariance and to take into consideration the relationship between adjacent pixels.

The Gaussian image pyramid is created by successively low-pass filtering and sub-sampling an image. During the stage of low-pass filtering the Gaussian function can be approximated by a discretized convolution kernel as follows:

$$\boldsymbol{G}_d = \frac{1}{256}\begin{bmatrix} 1 & 4 & 6 & 4 & 1 \\ 4 & 16 & 24 & 16 & 4 \\ 6 & 24 & 36 & 24 & 6 \\ 4 & 16 & 24 & 16 & 4 \\ 1 & 4 & 6 & 4 & 1 \end{bmatrix} \quad (2)$$

During sub-sampling every even-numbered row and column is removed. If we denote as I^o the original captured image and as I^ϕ the image at pyramid level ϕ then image at pyramid level $\phi+1$ is computed as: $I^{\phi+1}(x,y) = [\boldsymbol{G}_d * I^\phi](2x,2y)$

One must combine the various scales together into a single unified and scale-independent feature map, to provide scale-independent feature analysis. To do so, image at level $\phi+1$, firstly, is upsized twice in each dimension, with the new even rows and columns filled with zeros. Secondly, a convolution is performed with the kernel $\boldsymbol{G}_u$ to approximate the values of the "missing pixels". Because each new pixel has four non new-created adjacent pixels, $\boldsymbol{G}_u$ is defined as: $\boldsymbol{G}_u = 4 \cdot \boldsymbol{G}_d$.

Then, a pixel-wise weighted summation is performed to adjacent images in pyramid so as the unified image at level ϕ, J^ϕ is defined as:

$$J^\phi = \frac{1}{2} \cdot [I^\phi + [\boldsymbol{G}_u * U(I^{\phi+1})]] \quad (3)$$

where U stands for the upsize operation. The final unified image is computed by repeating the above operation, from coarser to finer pyramid image levels.

3.2 Low-level Features Analysis

As described in (Albrecht et al., 2011b) different low-level image features respond to different attributes of potential maritime targets. A combination of features should be exploited in order to reveal targets' presence. The selected features do not require a specific

format for the input image. These are edges, horizontal and vertical lines, frequency, color and entropy.

Each one of these features are calculated for all image's pyramid levels, independently. Then, image's pyramid is combined to form a single unified feature map by using Eq.(3). In Fig.2 the original captured frame along with the features responses are presented. All of the features emphasize the stationary land part and the white boat, which is the actual maritime target.

3.2.1 Edges

Edges in the form of horizontal and vertical lines are able to denote man-made structures, making the system able to suppress large image regions, depicting sea and sky. Canny operator (McIlhagga, 2011) is a very accurate image edge detector, which outputs zeros and ones for image edges absence and presence respectively. Sobel operator (Yasri et al., 2008), although being less accurate, measures the strength of detected edges by approximating the derivatives of intensity changes along image rows and columns.

So, by multiplying pixel-wise the output of two operators the system is able to detect edges in a very accurate way, while at the same time it preserves their magnitude. If we denote as C_I and S_I the Canny and Sobel operators for image I, then the edges $\mathcal{E}_I$ are defined as: $\mathcal{E}_I = C_I \cdot S_I$. Matrix $\mathcal{E}_I$ has the same dimensions with image I; its elements $\mathcal{E}_I(x,y)$ correspond to the magnitude of an image edge at location (x,y) on image plane.

3.2.2 Frequency

The high frequency components of the input frame, I, are computed as: $\mathcal{F}_I = \nabla^2 \cdot I$. The matrix $\mathcal{F}_I$ has the same dimensions with image I and its elements $\mathcal{F}_I(x,y)$ correspond to the frequency's magnitude at location (x,y) on image plane.

While exploitation of frequency features may emphasize (highly) wavy sea regions, they will suppress image regions that depict sky parts, since such image parts are dominated by low frequencies. Furthermore, image frequencies are complementary to image edges emphasizing highly structured regions within an object and thus improving detection accuracy.

3.2.3 Horizontal and Vertical Lines

The detection of horizontal and vertical lines in an image require an appropriate kernel K. Kernel K is tuned to strengthen the response of a pixel if this consists a part of a horizontal or vertical line and suppress pixels' responses in all other cases. Kernel will be convolved with each image's pyramid level. In order to emphasize this kind of lines the kernel K is designed as:

$$\boldsymbol{K} = \frac{1}{16}\begin{bmatrix} 0 & 0 & 1 & 0 & 0 \\ 0 & 0 & 2 & 0 & 0 \\ 1 & 2 & 4 & 2 & 1 \\ 0 & 0 & 2 & 0 & 0 \\ 0 & 0 & 1 & 0 & 0 \end{bmatrix} \tag{4}$$

and vertical and horizontal lines in a frame I can be computed as: $\mathcal{L}_I = \boldsymbol{K} * I$. Again, the matrix $\mathcal{L}_I$ has the same dimensions with image I and its elements $\mathcal{L}_I(x,y)$ indicates the magnitude of an horizontal and/or vertical line at location (x,y) on image plane.

Line detector works like an edge detector. In coastal regions, captured frames are likely to contains land parts that will respond to the edge detector, affecting detection accuracy of actual maritime targets. Since vertical and horizontal lines are more dominant in man-made structures the line detector supports accuracy of actual targets by suppressing the regions of the image that depict natural land parts, such as rocks.

3.2.4 Color

In maritime environment, no assumptions about the color of vessels can be made. For this reason differences in color are more likely to indicate the presence of a potential target. Furthermore, maritime scenes usually contain large regions with similar colors (sea and sky). This observation as described in (Achanta et al., 2009) and (Achanta and Susstrunk, 2010) can be exploited to increase the performance of visual attention map by identifying potential targets.

In order to compute the color difference, the captured frame's colorspace is converted to CIELab. The computation of color differences takes place by calculating the Euclidean distances between individual pixels color vectors and the mean color vector of the whole frame. For a frame I this procedure results in a matrix $\mathcal{C}_I$ of the same dimensions, whose element, $\mathcal{C}_I(x,y)$, at location (x,y) on image plane, indicates the difference in color between this pixel and the mean color of the rest pixels of the frame.

3.2.5 Entropy

Images that depict large homogeneous regions, such as sky or sea regions, present low entropy, while highly textured images will present high entropy. Image entropy can be interpreted as a statistical measure of randomness, which can be used to characterize the texture of the input image. Thus, entropy can be utilized to suppress homogeneous regions of sea and sky

and highlight potential maritime targets. Entropy, H_r, of a region r of an image is defined as:

$$H_r = \sum_{j=1}^{k} P_j^{(r)} \cdot \log P_j^{(r)} \quad (5)$$

where $P_j^{(r)}$ is the frequency of intensity j in image region r. For a grayscale image, variable k is equal to 256.

In order to compute entropy for a pixel located at (x,y) on image plane, we apply the relation of Eq.5 on a square window centered at (x,y). In our case, the size of the window is 5×5 pixels. The application of Eq.5 on (x,y) of a frame I, for $x = 1,...,w$ and $y = 1,...,h$, where w and h correspond to frame's width and height, results in a matrix $\mathcal{H}_I$ that has the same dimensions with the frame I. The matrix $\mathcal{H}_I$ can be interpreted as a pixel-wise entropy indicator of I.

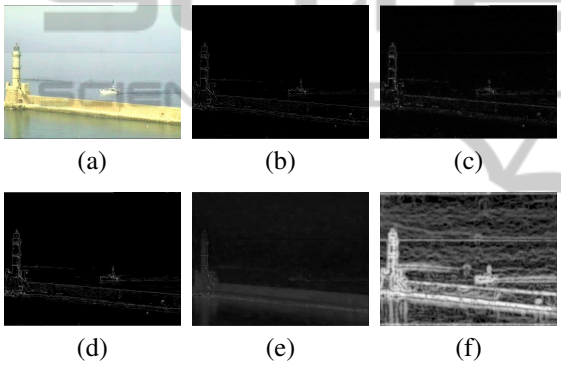

(a) (b) (c)

(d) (e) (f)

Figure 2: Original captured frame (a) and feature responses (b)-(f); (b) edges, (c) frequencies, (d) vertical and horizontal lines, (e) color and (f) entropy. All feature responded to the land part and the boat (maritime target).

3.3 Visual Descriptors

Visual descriptors are computed to encode visual information of captured images, using the extracted low-level features described in subsection 3.2. These descriptors are utilized for constructing the visual attention maps. Their computation, instead of pixel-wise, takes place block-wise, in order to reduce the effect of noisy pixels during low-level features extraction. In this paper, three different descriptors are computed:

a) *Local Descriptors* that take into consideration each one of the image pixels separately. Local descriptors indicate the magnitude of local features for each one of image pixels.

b) *Global Descriptors* that are capable to emphasize pixels with high uniqueness compared to the rest of the image. To achieve this they indicate how different local features for a specific pixel are, in relation with the same features of all other image pixels.

c) *Window Descriptors* that compare local features of a pixel with the same features of its neighboring pixels.

3.3.1 Local Descriptor

One local descriptor is computed for each one of the extracted low-level features. Let us denote as F the feature in question, which can correspond to image edges, frequency, horizontal and vertical lines, color or entropy. For the feature F, the computation of local descriptor is derived by feature's response image. Firstly the feature's response image is divided into B blocks of size 8×8 pixels. Then, the local descriptor for a specific block j is defined as the average magnitude of the feature F in the same block. More formally, for a block j, with b_h height and b_w width, the local descriptor of feature F is computed as follows:

$$lF_j = \frac{1}{b_h \cdot b_w} \sum_{(x,y) \in j} F(x,y) \quad (6)$$

where $F(x,y)$ is the response of feature in question at pixel (x,y). This kind of descriptor is capable to highlight image bocks with high feature responses.

3.3.2 Global Descriptor

The local descriptors handle each image block separately and, thus, are insufficient to provide useful information when features' responses are quite similar along all image blocks (e.g. a wavy sea). The proposed system can overcome this problem by using global descriptors. Uniqueness of a block j can be evaluated by the absolute difference of the feature response between this block and the rest blocks of the image. The global descriptor for a feature F and image block j is defined as:

$$gF_j = \frac{1}{B} \cdot \sum_{i=1}^{B} |lF_j - lF_i| \quad (7)$$

As mentioned before a global descriptor is able to emphasize blocks presenting high uniqueness, in term of features' responses, compared to the rest blocks of the image.

3.3.3 Window Descriptor

Unfortunately, if potential targets are presented in more than one block, the local and global descriptors will emphasize the most dominant target and will suppress the others. In order to overcome this problem,

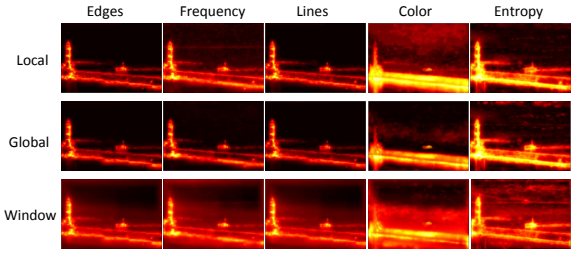

Figure 3: Visual attention maps for each local, global and window descriptors. Using give low level features and three descriptor, each one of the frames pixels is described by a 15-dimensional vector. The presented visual attention maps correspond to the original frame of Fig.2.

system exploits a window descriptor, that compares each image block with its neighbouring blocks.

Window descriptor for an image with $N \times M$ blocks uses an image window W, which is spanned by the maximum symmetric distance, d_h and d_v along horizontal and vertical axes respectively. Symmetric distances are defined as $d_h = min(l, k_h, N - k_h)$ and $d_v = min(l, k_v, M - k_v)$, where l is the default symmetric distance, 3 blocks in our case, and k_h and k_v stands for block coordinates on image plane along horizontal and vertical axes respectively. The window descriptor for a feature F and image block j with coordinates (j_1, j_2) is defined as:

$$wF_j = \frac{1}{2d_h \cdot 2d_v} \cdot \sum_{k=-d_h}^{d_h} \sum_{l=-d_v}^{d_v} |lF_j - lF_{j_1+k, j_2+l}| \quad (8)$$

By using three descriptors and five low-level image features, each image block is described by a 1×15 feature vector. Each feature of this vector corresponds to a different visual attention map. For blocks of size 8×8 pixels the visual attention maps are sixty four times smaller than the original captured frame. In order to create a pixel-wise feature vector, visual attention maps must have the same dimensions with the original captured frame. For this reason they are up-sampled, by using Eq.3.

Visual attention maps that correspond to the original frame of Fig.2, for each one of the descriptors and each one of the low level features, are presented in Fig.3. All visual attention maps emphasize the stationary land part and the boat, while at the same time they suppress the background.

3.4 Background Subtraction

In maritime surveillance, most state-of-the-art background modeling algorithms, like (Doulamis and Doulamis, 2012), (Makantasis et al., 2012), fail either due to their high computational cost or due to the continuously moving background, and moving cameras. However, if the background modeling algorithm output is fused in a unified feature vector with the previously constructed visual attention maps, our system will be able to emphasize potential threats and at the same time to suppress land parts that may be appeared in the scene by implicitly capture motion presence.

The proposed system uses the Mixtures of Gaussians (MOG) background modeling technique, presented in (Zivkovic, 2004). This choice is justified by the fact that MOG is fast, robust to small periodic movements of background, and easy to parameterize algorithm. By fusing together the outputs of visual attention maps and the output of a background modeling algorithm, camera motion temporarily increases false positives detections, but false negatives, that comprises the most important characteristic of a maritime surveillance system, are not affected.

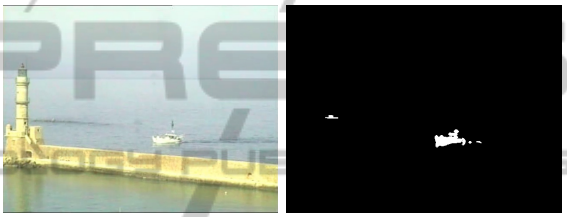

(a) (b)

Figure 4: Original frame (a) and the output of background modeling algorithm (b).

4 TARGET DETECTION

The maritime target detection can be seen as an image segmentation problem. In our case target detection, is further reduced to a binary classification problem. For any pixel at location (x, y) of a frame i, the feature extraction process (see Sec.3) constructs an 1×16 feature vector, $\boldsymbol{f}_{xy}^{(i)}$. Given $\boldsymbol{f}_{xy}^{(i)}$ as input, the classifier will decide if the corresponding pixel depicts some part of a maritime target or not.

4.1 Initial Training Set Formation

In order to be able to exploit a binary classifier, a process of classifier training should be preceded. Training process requires the formation of a robust training set which contains pixels along with their associated labels. Let us denote as $Z^{(t)}$ the set that contains all the pixels of frame t, $C_T^{(t)}$ the set that contains pixels that depict some part of a maritime target and as $C_B^{(t)}$ the set $Z^{(t)} - C_T^{(t)}$.

The creation of a training set S requires from the user to roughly segment the frame t into two regions, which contain positive and negative samples (i.e. pixels that belong to $C_T^{(t)}$ and $C_B^{(t)}$ class respectively).

This segmentation results in a set $S = \{(p_{xy}^{(t)}, l_{xy}^{(t)})\}$, and labels are defined as:

$$l_{xy} = \begin{cases} 1 & \text{if } p_{xy} \in C_T \\ -1 & \text{if } p_{xy} \in C_B \end{cases} \quad (9)$$

where p_{xy} is a pixel at location (x,y). By utilizing the feature vector $\boldsymbol{f}_{xy}^{(t)}$ the set S takes the form described in Sec.2.2.

However, human centric labeling, especially of image data, is an arduous and inconsistent task, mainly due to the complexity of the visual content and the huge manual effort required. To overcome this drawback, we refine the initial training set through a *semi-supervised* approach.

4.2 Training Set Refinement

In order to refine the initial user-defined training set, we partition the set S into two disjoint classes, R and U. The class R contains the most representative samples of S, i.e. the samples that can best describe the classes C_T and C_B, while class U is equal to $S-R$. Samples of class R are considered as labeled, while samples belonging to U are considered as unlabeled. Then, via a semi-supervised approach the samples of R are used for label propagation through the ambiguously labeled data of U. In the following we describe in detail the aforementioned process.

For selecting the most representative samples for each one of the classes C_T and C_B, we consider each sample as a point into an μ-dimensional space. Then, simplex volume expansion is utilized. In our case μ is equal to 16, because the dimension of the space is equal to the dimension of the feature vectors that describe the pixels. The process for representatives selection is conducted twice, once for class C_T and once for C_B.

4.3 Graph-based Label Propagation

The aforementioned procedure results to two sets of representative samples, $C_{T,R}$ and $C_{B,R}$, one for each class. The samples of $C_{T,R}$ and $C_{B,R}$ are considered as labeled, while the rest samples of the classes C_T and C_B are considered as ambiguously labeled. More formally, we have: i) $R = C_{T,R} \cup C_{B,R}$ and ii) $U = S - C_{T,R} - C_{B,R}$. At this point, we need to refine the initial training set, S, using a suitable approach for the label propagation, through the ambiguously labeled data.

Thus, we need to estimate a labeling prediction function $g : \mathbb{R}^{\mu} \mapsto \mathbb{R}$ defined on the samples of S, by using the labeled data R. Let us denote as $\boldsymbol{r}_i$ the samples of set R such as $R = \{\boldsymbol{r}_i\}_{i=1}^{m}$, where m is the cardinality of the set R. Then, according to (Liu et al., 2010), the label prediction function can be expressed as a convex combination of the labels of a subset of representative samples:

$$g(\boldsymbol{f}_i) = \sum_{k=1}^{m} Z_{ik} \cdot g(\boldsymbol{l}_k) \quad (10)$$

where Z_{ik} denotes sample-adaptive weights, which must satisfy the constraints $\sum_{k=1}^{m} Z_{ik} = 1$ and $Z_{ik} \geq 0$ (convex combination constraints). By defining vectors $\boldsymbol{g}$ and $\boldsymbol{\alpha}$ respectively as $\boldsymbol{g} = [g(\boldsymbol{f}_1), ..., g(\boldsymbol{f}_n)]^T$ and $\boldsymbol{\alpha} = [g(\boldsymbol{r}_1), ..., g(\boldsymbol{r}_m)]^T$. Eq.10 can be rewritten as $\boldsymbol{g} = \mathbf{Z}\boldsymbol{\alpha}$ where $\mathbf{Z} \in \mathbb{R}^{n \times m}$.

The design of matrix $\mathbf{Z}$, which measures the underlying relationship between the samples of U and representative samples R (were $R \subset U$), is based on weights optimization; actually non-parametric regression is being performed by means of data reconstruction with representative samples. Thus, the reconstruction for any data point $\boldsymbol{f}_i, i = 1, ..., n$ is a convex combination of its closest representative samples. In order to optimize these coefficients the following quadratic programming problem needs to be solved:

$$\begin{aligned} \min_{\boldsymbol{z}_i \in \mathbb{R}^s} \quad & h(\boldsymbol{z}_i) = \frac{1}{2} ||\boldsymbol{f}_i - \mathbf{R}_s \cdot \boldsymbol{z}_i||^2 \\ \text{s.t.} \quad & \mathbf{1}^T \boldsymbol{z}_i = 1, \boldsymbol{z}_i \geq 0 \end{aligned} \quad (11)$$

where, $\mathbf{R}_s \in \mathbb{R}^{\mu \times s}$ is a matrix containing as elements a subset of $R = \{\boldsymbol{r}_1, ..., \boldsymbol{r}_m\}$ composed of $s < m$ nearest representative samples of $\boldsymbol{f}_i$ and $\boldsymbol{z}_i$ stands for the i^{th} row of $\mathbf{Z}$ matrix.

Nevertheless, the creation of matrix $\mathbf{Z}$ is not sufficient for labeling the entire data set, as it does not assure a smooth function g. As mentioned before, a large portion of data are considered as ambiguously labeled. Despite the small labeled set, there is always the possibility of inconsistencies in segmentation; in specific frames the user may miss some pixels that depict targets. In order to deal with such cases the following SSL framework is employed:

$$\min_{\boldsymbol{A}=[\boldsymbol{\alpha}_1, ..., \boldsymbol{\alpha}_c]} Q(\mathbf{A}) = \tfrac{1}{2} ||\mathbf{Z} \cdot \mathbf{A} - \mathbf{Y}||_F^2 + \tfrac{\gamma}{2} trace(\mathbf{A}^T \hat{\mathbf{L}} \mathbf{A}) \quad (12)$$

where $\hat{\mathbf{L}} = \mathbf{Z}^T \cdot \mathbf{L} \cdot \mathbf{Z}$ is an memory-wise and computationally tractable alternative of the Laplacian matrix $\mathbf{L}$. The matrix $\mathbf{A} = [\boldsymbol{a}_1, ..., \boldsymbol{a}_c] \in \mathbb{R}^{m \times c}$ is the soft label matrix for the representative samples, in which each column vector accounts for a class. The matrix $\mathbf{Y} = [\boldsymbol{y}_1, ..., \boldsymbol{y}_c] \in \mathbb{R}^{n \times c}$ a class indicator matrix on ambiguously labeled samples with $Y_{ij} = 1$ if the label l_i of sample i is equal to j and $Y_{ij} = 0$ otherwise.

In order to calculate the Laplacian matrix $\mathbf{L}$, the adjacency matrix $\mathbf{W}$ needs to be calculated, since $\mathbf{L} = \mathbf{D} - \mathbf{W}$, where $\mathbf{D} \in \mathbb{R}^{n \times n}$ is a diagonal degree

matrix such that $\mathbf{D}_{ii} = \sum_{j=1}^{n} \mathbf{W}_{ij}$. In this case $\mathbf{W}$ is approximated as $\mathbf{W} = \mathbf{Z} \cdot \mathbf{\Lambda}^{-1} \cdot \mathbf{Z}^T$, where $\mathbf{\Lambda} \in \mathbb{R}^{m \times m}$ is defined as: $\Lambda_{kk} = \sum_{i=1}^{n} Z_{ik}$. The solution of the Eq.12 has the form of: $\mathbf{A}^* = (\mathbf{Z}^T \cdot \mathbf{Z} + \gamma \hat{\mathbf{L}})^1 \mathbf{Z}^T \mathbf{Y}$. Each sample label is, then, given by:

$$\hat{l}_i = arg \max_{j \in \{1,\ldots,c\}} \frac{\mathbf{Z}_i \cdot \boldsymbol{\alpha}_j}{\lambda_j} \tag{13}$$

where $\mathbf{Z}_i. \in \mathbb{R}^{1 \times m}$ denotes the i-th row of $\mathbf{Z}$, and the normalization factor$\lambda_j = \mathbf{1}^T \mathbf{Z} \boldsymbol{\alpha}_j$ balances skewed class distributions.

4.4 Maritime Target Detection

Having constructed a training set, $S = \{\boldsymbol{f}_i, l_i\}_{i=1}^{n}$, a binary classifier, capable to discriminate pixels that depict some part of a maritime target from pixels that depict the background, can be trained. In this paper we choose to utilize Support Vectors Machine (SVM) to transact the classification task. The optimization problem is described as (Cortes and Vapnik, 1995):

$$\begin{aligned} &\min_{\tilde{\boldsymbol{w}}, b, \boldsymbol{\xi}} \frac{1}{2} ||\boldsymbol{w}|| + c \sum_{i=1}^{n} \xi_i \\ &\text{s.t. } l_i(\boldsymbol{w} \cdot \boldsymbol{f}_i - b) \geq 1 - \xi_i \end{aligned} \tag{14}$$

for $i = 1, \ldots, n$, $\xi_i \geq 0$. Where $\xi_i \geq 1$ are variables that allow a sample to be in the margin or to be misclassified and c is a constant that weights these errors.

In the framework of maritime detection, SVM must be able to handle unbalanced classification problems, due to the fact that maritime target usually occupy the minority of captured frames' pixels let alone their total absence from the scene for large time periods. To address this problem, the misclassification error for each class is weighted separately. This means that the total misclassification error of Eq.14 is replaced with two terms:

$$c \sum_{i=1}^{n} \xi_i \rightarrow c_p \sum_{\{i|l_i=1\}} \xi_i + c_n \sum_{\{i|l_i=-1\}} \xi_i \tag{15}$$

where c_p and c_n are constant variables that weight separately the misclassification errors for positive and negative examples. The solution of Eq.14 with the classification error of Eq.15 results to a trained SVM, which is capable to classify the pixels of new captured frames.

5 EXPERIMENTAL RESULTS

There is code in Python, concerning visual attention maps construction, available to download[1]. The performance of each system's component have been checked separately; extracted features were evaluated in terms of discriminative ability and importance, semi-supervised labeling for the predicting outcome and, finally, the binary classifier for its performance.

5.1 Data Set Description

Data consists of recorded videos from cameras mounted at the Limassol port, Cyprus and Chania old port, Crete, Greece. The data sets describe real life scenarios, in various weather conditions. As long as the camera is able to capture a vessel (i.e. spans an area of more than 40 pixels in the frame) the system will likely detect it, regardless the weather conditions (e.g. rain, fog, waves etc.).

Unfortunately, for the vast majority of the video frames, maritime targets are absent from the scene. In order to deal with such cases, we manually edited the videos and kept only the tracks that depict intrusion of one or more targets in the scene. Then, we manually labeled the pixels of key video frames, *keyframes*, to create a ground truth dataset for evaluating our system.

Keyframes originate from raw video frames that correspond to time instances $t, 2t, 3t, \cdots$ The time span is selected to be 6 seconds, which means that one frame out of 150 is denoted as keyframe. We followed this approach for practical reasons. Firstly, it would be impossible to manually label all video frames at a framerate of 25 fps. Also, the time interval of 6 seconds is small enough to allow the detection of the intrusion of a maritime target in the scene. At this point it has to be clarified that feature extraction task, as well as the binary classification are performed for all frames of a video track. Keyframes are used only for system's performance evaluation.

5.2 Evaluation of Extracted Features

In this section, we examine if extracted features fulfil specific requirements, i.e. be informative and separable, in order to assure good classification accuracy and smooth training set refinement, through the graph based SSL technique.

To evaluate features information, we utilized the keyframes' ground truth data. The feature extraction task results in a 16-dimensional feature vector for each pixel in a frame. The quality of features' information is evaluated through dimensionality reduction and samples plotting, in order to visually examine their distribution in space, see Fig.5. The two classes, as shown in Fig.5, are linearly separable, which suggests high quality features. The small amount of pos-

[1] https://github.com/konstmakantasis/Poseidon

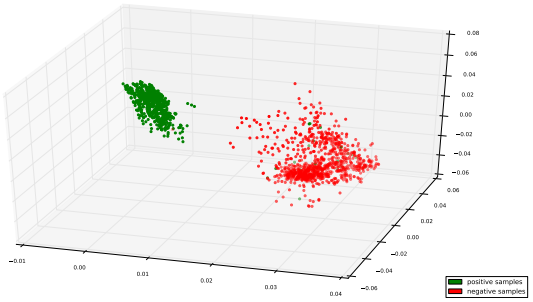

Figure 5: Positive and negative samples plotted in 3-dimensional space. Randomized PCA was used to extract the three dominant components of the dataset. The class containing positive samples can be linearly separated from the class containing negative samples. The small amount of positive samples that lie inside the region of the negative class, correspond to maritime targets' contours.

itive samples, that lie inside the region of the negative class, correspond to maritime targets' contours and probably occurred due to segmentation errors during manual labeling.

The importance of each one of the extracted features is examined separately, in order to define how much each one of the features affects the classification task. The importance of features is specified via Forest of Randomized Trees. The relative rank (i.e. depth) of a feature used as a decision node in a tree can be used to assess the relative importance of that feature with respect to the predictability of the target variable. Features used at the top of the tree contribute to the final prediction decision of a larger fraction of the input samples. The expected fraction of the samples they contribute to can thus be used as an estimate of the relative importance of the features.

In Fig.6 the relative importance of each one of the extracted features is presented (features labeling follows the notation of Section 3). The dominant feature is the one that corresponds to the output of background modeling algorithm, which, in practice, captures the presence of motion in the scene. The rest of the features contribute almost the same, except from the feature that corresponds to the local descriptor of image entropy.

5.3 Evaluation of Semi-supervised Labeling

In order to evaluate semi-supervised labeling, we assume that manual labeling of keyframes contains no segmentation errors. The ratio of the representatives samples in relation with the ambiguously labeled samples is the only factor that affect the performance of labeling algorithm.

As shown in Fig.7, the labeling error is lower than

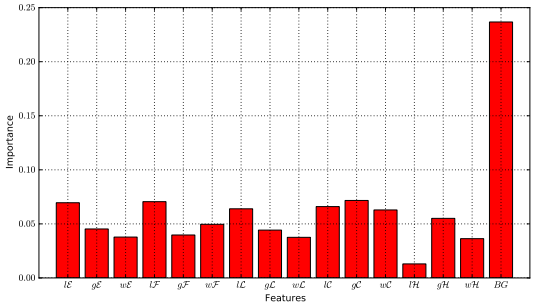

Figure 6: Features importances. The feature that corresponds to output of background modeling algorithm, which implicitly captures the presence of motion in the scene, is presented to be he most important.The rest of the features contribute almost the same to the classification task, except from the feature that corresponds to the local descriptor of image entropy, which presents the lowest importance.

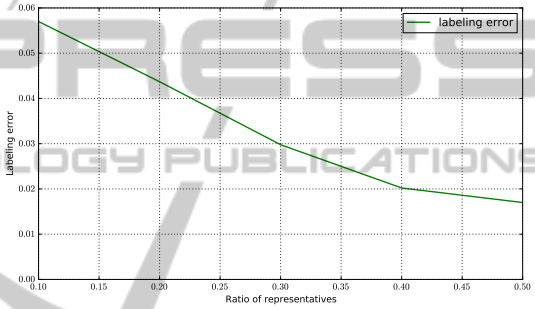

Figure 7: Semi-supervised labeling performance. When ratio of representative samples is over 40% the labeling error is lower than 2%. When the ratio of representatives is lower than 40% the error is linearly increasing till the value of 5.7% for 10% of representatives.

2% when the ratio of the representatives samples in relation with the ambiguously labeled samples is over 40%. When the ratio is smaller than 40% the labeling error is linearly increasing and it reaches the value of 5.7% when the ratio of representative samples is 10%.

The choice for an appropriate value for the ratio of representatives is inherently dependent on the quality of human based labeling. If labeling is the result of a rough image segmentation, a lot of the labeled pixel will carry the wrong label. In such cases the aforementioned ratio must be set to a small value. The most representative samples from each class is assumed that carry the right label, while the labels of the rest of the samples must be reconsidered.

In our case, we ask the user to segment the frame in a very careful way, which implies that the vast majority of the pixels will carry the right label. For this reason we set the ratio value to 40%. The semi-supervised labeling algorithm with 40% of representatives is expected to re-label 1.7% of the samples.

5.4 Binary Classifier Evaluation

The performance of the binary classifier is dependent on the values of the parameters c_p and c_n of Eq.15. Let us denote as n_p and n_n the number of samples in positive and negative class respectively. To examine the influence of parameters c_p and c_n on classification accuracy we define the parameter k as:

$$k = \frac{c_n \cdot n_n}{c_p \cdot n_p} \tag{16}$$

In practice, parameter k assigns different weights to misclassification errors, which correspond to positive and negative examples. When the value of k is equal to one, the weights that penalize misclassification sample for each class are inversely proportional to the cardinalities of the classes. When $k < 1$ a bigger penalty is assigned to false negatives, while for $k > 1$ false positives are considered more important. False negatives correspond to pixels that actually depict some part of a maritime target, but are denoted as background by the classifier.

However, a maritime surveillance system must emphasize on minimizing the false negative rate. In other words, it is more important, the system to detect all potential maritime targets, even if it will raise a small amount of false alarms, than minimizing false positives at the cost of missing target intrusions.

Fig.8 presents the performance of classifier for different values of parameter k. The green line represents classification accuracy, while the blue line the recall of the system. If we denote as p_c the set of pixel that denoted by the classifier as positive samples and as p_t the set of pixels that actually belong to the positive class, then recall ρ is defined as:

$$\rho = \frac{p_c \cap p_t}{p_t} \tag{17}$$

When ρ is equal to one, all true positive samples have been correctly classified by the binary classifier. Accuracy is the proportion of correctly classified samples of the whole dataset. As shown by the green line in Fig.8 the accuracy of the classifier reaches its maximum value, when k is equal to one. On the other hand, the recall of the system is monotonically decreasing as the value of k is increasing. In our case we set $k = 0.7$ to balance between maximizing classification accuracy and minimizing false negative rate. For $k = 0.7$ the accuracy of the classifier is equal to 96.4%, while recall is equal to 97.1%.

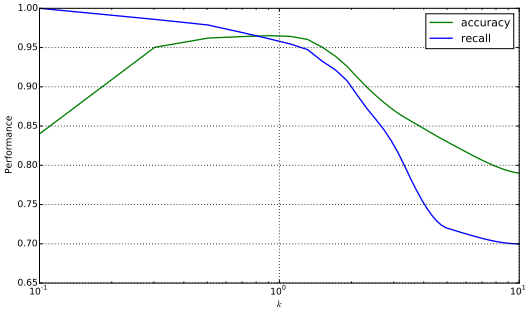

Figure 8: Classifier performance. The recall of the system is monotonically decreasing as the value of k is increasing (blue line). The accuracy presents the maximum value when $k = 1$, which means that the penalties for misclassifying positive and negative samples are inversely proportional to the cardinalities of positive and negative classes.

6 CONCLUSIONS

A vision based system, using monocular camera data, is presented in this paper. The system provides robust results by combining supervised and unsupervised methods, appropriate for maritime surveillance, utilizing an innovative initialization procedure. The system offline initialization is achieved through graph based SSL algorithm, suitable for large data sets, supporting users during segmentation process.

Extensive performance analysis suggest that the proposed system performs well, in real time, for long periods without any special hardware requirements and the without any assumptions related to scene, environment and/or visual conditions. Such system is expected to be easily expanded to other surveillance cases, using minor modifications depending on the case.

ACKNOWLEDGEMENTS

The research leading to these results has been supported by European Union funds and National funds (GSRT) from Greece and EU under the project JASON: Joint synergistic and integrated use of eArth obServation, navigatiOn and commuNication technologies for enhanced border security funded under the cooperation framework. The work has been partially supported by IKY Fellowships of excellence for postgraduate studies in Greece−Siemens program.

REFERENCES

Achanta, R., Hemami, S., Estrada, F., and Susstrunk, S. (2009). Frequency-tuned salient region detection. In *IEEE Conf. on Comp. Vis. and Pat. Rec., 2009. CVPR 2009*, pages 1597–1604.

Achanta, R. and Susstrunk, S. (2010). Saliency detection using maximum symmetric surround. In *2010 17th*

IEEE Int. Conf. on Image Processing (ICIP), pages 2653–2656.

Albrecht, T., Tan, T., West, G., Ly, T., and Moncrieff, S. (2011a). Vision-based attention in maritime environments. In *Communications and Signal Processing (ICICS) 2011 8th Int. Conf. on Information*,pages 1–5.

Albrecht, T., West, G., Tan, T., and Ly, T. (2010). Multiple views tracking of maritime targets. In *2010 Int. Conf. on Digital Image Computing: Techniques and Applications (DICTA)*, pages 302–307.

Albrecht, T., West, G., Tan, T., and Ly, T. (2011b). Visual maritime attention using multiple low-level features and na #x0ef;ve bayes classification. In *2011 Int. Conf. on Digital Image Computing Techniques and Applications (DICTA)*, pages 243–249.

Alexe, B., Deselaers, T., and Ferrari, V. (2010). What is an object? In *2010 IEEE Conf. on Comp. Vis. and Pat. Rec. (CVPR)*, pages 73–80.

Auslander, B., Gupta, K. M., and Aha, D. W. (2011). A comparative evaluation of anomaly detection algorithms for maritime video surveillance. volume 8019, pages 801907–801907–14.

Belkin, M. and Niyogi, P. (2002). Using manifold structure for partially labelled classification. page 929.

Cortes, C. and Vapnik, V. (1995). Support-vector networks. *Machine Learning*, 20(3):273–297.

Doulamis, N. and Doulamis, A. (2012). Fast and adaptive deep fusion learning for detecting visual objects. In Fusiello, A., Murino, V., and Cucchiara, R., editors, *Comp. Vis. ECCV 2012. Workshops and Demonstrations*, number 7585 in Lecture Notes in Computer Science, pages 345–354. Springer Berlin Heidelberg.

Fischer, Y. and Bauer, A. (2010). Object-oriented sensor data fusion for wide maritime surveillance. In *Waterside Security Conf. (WSS), 2010 Int.*, pages 1–6.

Kaimakis, P. and Tsapatsoulis, N. (2013). Background modeling methods for visual detection of maritime targets. In *Proceedings of the 4th ACM/IEEE Int. Workshop on Anal. and Retrieval of Tracked Events and Motion in Imagery Stream*, ARTEMIS '13, pages 67–76, New York, NY, USA. ACM.

Lei, P.-R. (2013). Exploring trajectory behavior model for anomaly detection in maritime moving objects. In *2013 IEEE Int. Conf. on Intelligence and Security Informatics (ISI)*, pages 271–271.

Liu, T., Yuan, Z., Sun, J., Wang, J., Zheng, N., Tang, X., and Shum, H.-Y. (2011). Learning to detect a salient object. *IEEE Trans. on Pat. Anal. and Machine Intelligence*, 33(2):353–367.

Liu, W., He, J., and Chang, S.-F. (2010). Large graph construction for scalable semi-supervised learning. In *Proceedings of the 27th Int. Conf. on Machine Learning (ICML-10)*, pages 679–686.

Makantasis, K., Doulamis, A., and Doulamis, N. (2013). Vision-based maritime surveillance system using fused visual attention maps and online adaptable tracker. In *2013 14th Int. Workshop on Image Anal. for Multimedia Interactive Services (WIAMIS)*,pages 1–4.

Makantasis, K., Doulamis, A., and Matsatsinis, N. (2012). Student-t background modeling for persons' fall detection through visual cues. In *2012 13th Int. Workshop on Image Anal. for Multimedia Interactive Services (WIAMIS)*, pages 1–4.

Maresca, S., Greco, M., Gini, F., Grasso, R., Coraluppi, S., and Horstmann, J. (2010). Vessel detection and classification: An integrated maritime surveillance system in the tyrrhenian sea. In *2010 2nd Int. Workshop on Cognitive Information Processing (CIP)*,pages 40–45.

McIlhagga, W. (2011). The canny edge detector revisited. *Int. Journal of Comp. Vis.*, 91(3):251–261.

Nadler, B., Srebro, N., and Zhou, X. (2009). Statistical analysis of semi-supervised learning: The limit of infinite unlabelled data. In Bengio, Y., Schuurmans, D., Lafferty, J. D., Williams, C. K. I., and Culotta, A., editors, *Advances in Neural Information Processing Systems 22*, pages 1330–1338. Curran Associates, Inc.

Nilsson, M., van Laere, J., Ziemke, T., and Edlund, J. (2008). Extracting rules from expert operators to support situation awareness in maritime surveillance. In *2008 11th Int. Conf. on Information Fusion*,pages 1–8.

Rodriguez Sullivan, M. D. and Shah, M. (2008). Visual surveillance in maritime port facilities. volume 6978, pages 697811–697811–8.

Socek, D., Culibrk, D., Marques, O., Kalva, H., and Furht, B. (2005). A hybrid color-based foreground object detection method for automated marine surveillance. In Blanc-Talon, J., Philips, W., Popescu, D., and Scheunders, P., editors, *Advanced Concepts for Intelligent Vision Systems*, number 3708 in Lecture Notes in Computer Science, pages 340–347. Springer Berlin Heidelberg.

Szpak, Z. L. and Tapamo, J. R. (2011). Maritime surveillance: Tracking ships inside a dynamic background using a fast level-set. *Expert Systems with Applications*, 38(6):6669–6680.

Vandecasteele, A., Devillers, R., and Napoli, A. (2013). A semi-supervised learning framework based on spatio-temporal semantic events for maritime anomaly detection and behavior analysis. In *Proceedings CoastGIS 2013 Conf.: Monitoring and Adapting to Change on the Coast*.

Voles, P. (1999). Target identification in a complex maritime scene. volume 1999, pages 15–15. IEE.

Wijnhoven, R., van Rens, K., Jaspers, E., and de With, P. (2010). Online learning for ship detection in maritime surveillance. pages 73–80.

Yasri, I., Hamid, N., and Yap, V. (2008). Performance analysis of FPGA based sobel edge detection operator. In *Int. Conf. on Electronic Design, 2008. ICED 2008*, pages 1–4.

Zemmari, R., Daun, M., Feldmann, M., and Nickel, U. (2013). Maritime surveillance with GSM passive radar: Detection and tracking of small agile targets. In *Radar Symposium (IRS), 2013 14th Int.*, volume 1, pages 245–251.

Zhu, X. (2003). Semi-supervised learning using gaussian fields and harmonic functions. In *Proceedings of the 20th Int. Conf. on Machine learning (ICML-2003)*, volume 20, page 912.

Zivkovic, Z. (2004). Improved adaptive gaussian mixture model for background subtraction. In *Proceedings of the 17th Int. Conf. on Pat. Rec., 2004. ICPR 2004*, volume 2, pages 28–31 Vol.2.